Experimental study of particle-turbulence interaction in homogeneous turbulence

Alec Petersen

Department of Aerospace Engineering & Mechanics
St. Anthony Falls Laboratory
University of Minnesota
2 SE 3rd Ave, Minneapolis, MN 55414
pet00105@umn.edu

Luci Baker

Department of Aerospace Engineering & Mechanics
University of Minnesota
110 Union Street Se
Minneapolis, MN, 55455
bake0616@umn.edu

Doug Carter

Department of Aerospace Engineering & Mechanics
St. Anthony Falls Laboratory
University of Minnesota
2 SE 3rd Ave, Minneapolis, MN 55414
carte775@umn.edu

Filippo Coletti

Department of Aerospace Engineering & Mechanics
University of Minnesota
St. Anthony Falls Laboratory
110 Union Street Se
Minneapolis, MN, 55455
fcoletti@umn.edu

ABSTRACT

We study the clustering and settling of inertial particles in a novel experimental facility designed to produce a large region of homogeneous turbulence. Using two-dimensional particle-imaging velocimetry (PIV) and particle-tracking velocimetry (PTV), we explore particle-turbulence coupling through the full range of scales from Kolmogorov up to the integral length scale. We find particle clusters using Voronoï tesselation. These clusters are self similar, as indicated by their fractal nature and the power-law decay of their area distribution. The size of these clusters extends to the limits of our field of view, 30 cm in length, indicating the multiscale physics involved in preferential concentration. We also find that particles with Stokes number near one have the highest increase in settling velocity, up to almost three times the still-fluid value. We find further evidence that this is due to preferential sweeping, and that the effect is stronger for clustered particles. Finally, we present some evidence of inertial particles increasing the turbulent kinetic energy of the fluid phase, even for relatively modest volume fractions.

Introduction

Volcanic eruptions, raindrop formation in clouds and desert dust storms are tied together by their common physics — the complex, coupled interaction between a dense dispersed phase and a turbulent carrier fluid. Knowing how these inertial particles spread through the environment, settle to the ground, collide or agglomerate, and even affect the carrier-phase turbulence all depends on our understanding of that coupling. For particles both denser than the carrier fluid and sub-Kolmogorov in size, the relevant parameter for describing that coupling is the Stokes number $St_\eta = \tau_p/\tau_\eta$, the ratio between the aerodynamic particle response time $\tau_p = \rho_p d_p^2/18\mu$ and the Kolmogorov time scale. For particles with $St_\eta \approx 1$, neither the fluid nor the particle inertia dominates the interaction between the two, leading to some remarkable behaviors. One of the most studied among those is preferential concentration, thought to affect phenomenon ranging from the collisional growth of raindrops (Grabowski & Wang 2013) to the dust agglomeration in protoplanetary disks (Cuzzi *et al.* 2001).

Maxey (1987) provided the first explanation for preferential concentration, in which the smallest-scale (the Kolmogorov length η) eddies centrifuge particles out of their cores and into high-strain regions where the particles accumulate. More recent studies have pointed to the multiscale nature of particle clustering (Goto & Vassilicos, 2006) and proposed alternative mechanisms (Goto & Vassilicos, 2008; Bragg & Collins 2014), yet there are some features of clustering that are agreed upon. No matter the mechanism, clustering seems to reach a maximum for $St_\eta \approx 1$ particles (Wang & Maxey 1993, Eaton & Fessler 1994) and also has important consequences on particle collision rates (Sundaram & Collins 1997), and acceleration statistics (Bec *et al.* 2006).

Turbulence also influences how fast particles fall through turbulence when in a gravitational field. Wang & Maxey (1993) demonstrated that turbulence can increase the settling velocity of small inertial particles beyond their terminal velocity. In their proposed mechanism—preferential sweeping—particle trajectories favor the downward arc of turbulent eddies. Measurements by Aliseda *et al.* (2002), Yang & Shy (2003,2005) confirmed this phenomenon, which is also most pronounced for particles with $St_\eta \approx 1$. Less common are studies claiming reduced settling velocity due to turbulence (Nielsen 1993; Tooby *et al.* 1977). Simulations by Good *et al.* (2014) suggest that reduced settling velocity is only possible in direct numerical simulations when nonlinear drag is at play.

For sufficiently high concentrations, the particles can also back-react on the fluid phase and modify the turbulence itself (two-way coupling). Most studies concerned with this regime simulate the effect of particle loading in a zero-gravity environment, consistently finding turbulent kinetic energy attenuation for particles smaller than η and with $St_\eta \approx 1$ (Elghobashi & Truesdell 1993; Poelma *et al.* 2007). However, in the presence of gravity, turbulence can in fact be enhanced by fast-falling particles (Yang & Shy 2005, Frankel *et al.* 2016).

Our understanding of particle-turbulence dynamics is hindered by the scarcity of experimental data, which is partially due to the difficulty of generating large scale homogeneous turbulence. Grid

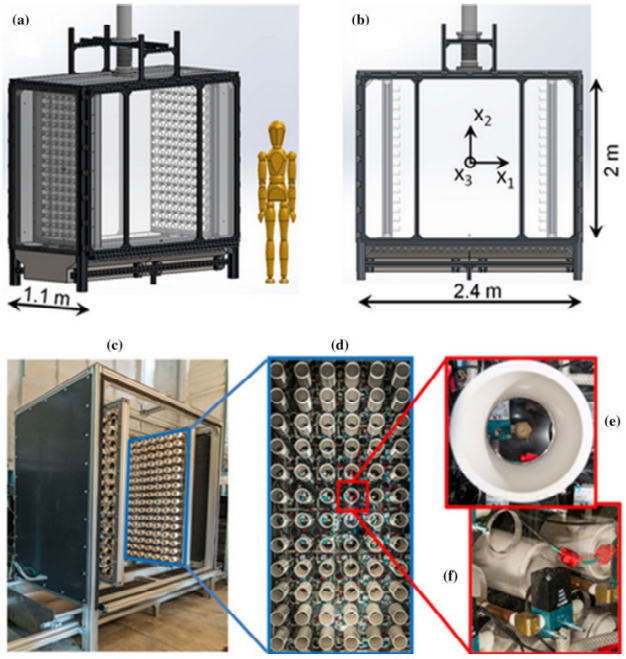

Figure 1. Isometric (**a**) and frontal (**b**) views of the installation. Photo of build (**c**) with close-up on one jet array (**d**) and an individual nozzle (**e**) and a rear view of an actuation valve (**f**).

turbulence in wind tunnels can produce large Reynolds numbers but with strong mean flow and significant streamwise decay of turbulent kinetic energy. Most stirred-tank facilities designed to generate turbulence without mean flow often have substantial recirculation and inhomogeneities. Turbulence boxes, with jets, loudspeakers or fans pointed centrally are effective at generating turbulence with good homogeneity and isotropy, but the region over which this occurs is small, usually smaller than the integral length scale. Therefore the suspended particles cannot interact with the full range of turbulent scales while traversing the homogeneous region, raising the question of how the turbulence forcing could be affecting the particle dynamics. In this study, we present two-phase measurements of particle-turbulence coupling, carried out in a novel facility designed to address these limitations

Methods

Inspired by the design of Bellani & Variano (2014), we built a similar apparatus (figure 1) to generate turbulence in air rather than water. Our variant, described in detail by Carter *et al.* (2016), generates air turbulence in a 2.4 x 2 x 1.1 m^3 volume via two facing jet arrays. These arrays are able to slide within the chamber and accommodate arrays of 8 by 16 ports each, fed by air pressurized at 800 kPa. Air flow through the 256 ports is controlled by solenoid valves, each individually actuated by a reconfigurable input/output system (NI cRio-9066). The valve outlets are connected to 5 cm-long copper tubes (10mm inner diameter) terminating with straight brass nozzles. These produced chocked jets of small mass flux, which entrain most of the flow rate from the surrounds, at a ratio of 50:1. Because only 2% of the effective mass flow rate comes from the pressurized air, we avoid both pressurizing the chamber and limit the formation of unwanted recirculating motions.

We force the turbulence with Variano & Cowen's (2008) sunbathing algorithm, in which the time each valve is open or closed is chosen from a specified Gaussian distribution. This "on time" is the main forcing parameter we use to change the intensity of our turbulence. By varying it from 50 ms to 10 s, we can generate turbulence with a range of Re_λ from 200 to 500, while keeping the flow homogeneous and the mean flow minimal. The integral length scale and the rms velocity fluctuations are on the order of 0.1 m and 1 m/s respectively.

We perform PIV and PTV measurements along the x_1-x_2 symmetry plane in the center of the chamber using 1-2 μm DEHS droplets as seeding. We use various inertial particles for our multiphase experiments including 30 μm lycopodium spores (1.2 g/cc), 29, 52 and 96 μm glass spheres (2.5 g/cc) and 95 μm glass bubbles (0.1 g/cc). Based on their properties and the turbulence characteristics we define for them Stokes number St_η in the range of 0.4—17 and Sv_η from 0.3 to 7. Here Sv_η is defined as the ratio of particle terminal velocity, $\tau_p g$ and the Kolmogorov velocity scale v_η. These particles descend through a 3-meter chute at the top of the chamber, assuring that they reach terminal velocity before entering the measurement region. Our imaging system includes a dual-head Nd:YAG laser (Big Sky, 532 nm) synchronized with a TSI CCD camera. We took images at two different zooms, one a 15x15 cm^2 window, the other 30x30 cm^2, with velocity vector resolutions of 4 and 9 η respectively. To perform multiphase flow measurements, we use size and intensity thresholds to separate tracers from inertial particles (Kiger & Pan (2000), Khalitov & Longmire (2002)), which are then analyzed by PIV and PTV respectively. Our PIV algorithm is a standard multi-pass FFT based cross correlation (Nemes *et al.* (2015)) with window offset and deformation. We also use a cross-correlation based particle-tracking algorithm inspired by Hassan *et al.* (1992).

Clustering

Following Monchaux *et al.* (2010), we use Voronoï tessellation to identify local particle concentration in our images. One of the advantages of this method is that concentration thresholds for a particle to belong to a cluster is intrinsic to the specific distribution, rather than being chosen *a priori*. Probability density functions for Voronoï cell area (normalized by the average cell area $\langle A_V \rangle$)are shown in figure 2 for the various clustering experiments.

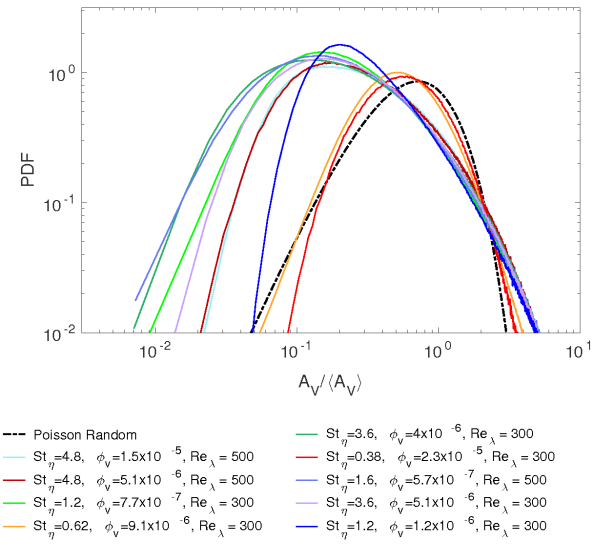

Figure 2. PDF of the Voronoï cell area A_V normalized by the mean cell area $\langle A_V \rangle$ for each case.

By comparing the Γ distribution of Voronoï areas expected for homogeneously distributed particles (Ferenc & Néda, 2007); the in-

tersections above and below the mean area define the thresholds for voids and clusters respectively.

As discussed by Baker *et al.*(Submitted), this alone is not a sufficient condition to establish which particles are clustered. Firstly, clusters are formed by particles whose Voronoi celss form a connected set. Secondly, since preferential concentration is driven by the underlying turbulence, coherent clusters should have topological features reflecting those dynamics.

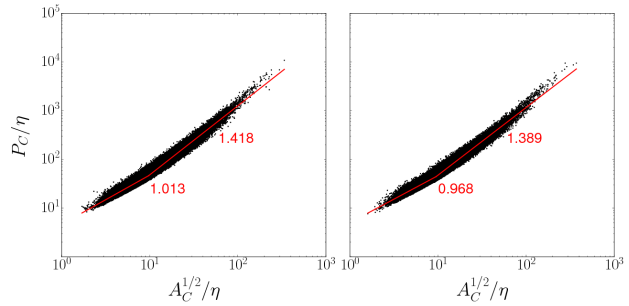

Figure 3. Cluster perimeter vs. the square root of cluster area for the (left) $Re_\lambda = 300$, $St_\eta = 1.21$, $Sv_\eta = 0.98$, $\phi_v = 7.72e-6$ case, and (right) the $Re_\lambda = 500$, $St_\eta = 1.53$, $Sv_\eta = 0.87$, $\phi_v = 5.7e-7$ case.

Both turbulent fields (Sreenivasan, 1991) and inertial particles (Goto & Vassilicos, 2006) in turbulence exhibit some degree self-similarity and fractal patterns leading Baker *et al.*(Submitted) to impose a futher restriction that the clusters be large enough to display self-similarity. Figure 3 shows the relationship between the perimeter of a set of connected Voronoï cells and the square root of its area. For small clusters, the relationship follows a power law with an exponent of approximately 1 (expected for regular two-dimensional objects) while larger clusters exhibit an exponent of 1.4, indicating their more space filling and fractal nature. The PDFs of cluster volumes (figure 4) further supports the self-similar behavior as the distributions consistently follow a power law above a certain area threshold which can be quite extensive, even multiple decades for the higher St_η cases. The slope is close to -2, found experimentally by Monchaux *et al.* (2010) among others.

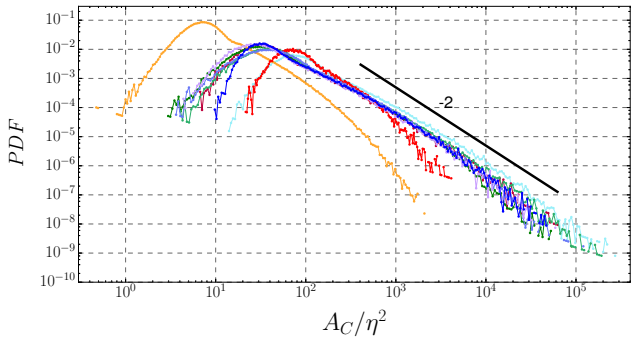

Figure 4. PDFs of cluster area normalized by the Kolmogorov area, η^2. Color code as in figure 2.

Figure 4 also shows that particle clusters can be extremely large. Clusters regularly surpass 10^4 η^2, with some even extending beyond 10^5. An example of such a "megacluster" is shown in figure 5, with a vertical length of at least 30 cm, though it is possible that the cluster size is limited by our field of view. Such a large structure suggests to the multiscale nature of clustering mechanisms. However in dense particle fields such as in figure 5, it is difficult to obtain reliable fluid-phase information so we are so far unable to confirm what topological features of the fluid affect such large-scale clustering, with Goto & Vassilicos's (2008) sweep-stick mechanism being one possible explanation. This megacluster also stands out for having such an irregular, porous shape—though that can perhaps be attributed to our laser sheet taking a cross-sectional slice from the three-dimensional structure.

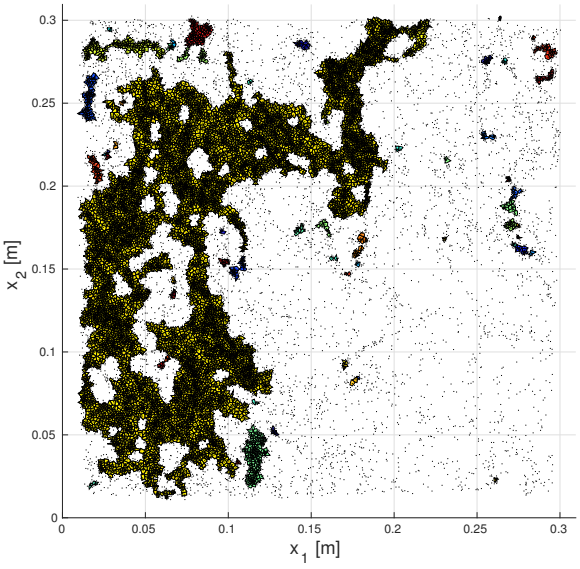

Figure 5. Instantaneous 2D slice of a mega-cluster ∼30 cm in length.

We also investigated how the particle concentration varies with cluster size. Figure 6 shows how the cluster area scales with the particle count inside each cluster. A least-squares fitting suggests a power law with exponent near one, meaning that the mean concentration is approximately constant throughout the whole range of cluster sizes, i.e. it does not depend on the cluster size but only on the set of physical parameters.

Table 1 lists the parameters for our clustering experiments, including the mean ratio between the mean cluster concentration $\langle C_C \rangle$ and the overall particle concentration C_0, and the mean cluster area normalized by η^2. The cluster concentration ranges from about four to ten times greater than the full domain concentration. As expected, particles with St_η close to unity are the most clustered. However the picture is complicated by the fact that unlike simulations using point particles, ours have finite sizes. This could potentially impact how dense particles like the glass bubbles with $d_p = 92\mu$m can get. Our cases with $St_\eta > 1$ exhibit a trend found by others, (Bec *et al.*, 2014; among others) that gravitational settling increases the in-cluster concentration, although the mechanism is still unclear. We also find that the mean cluster size generally increases with St_η and Sv_η, although finite particle size certainly plays a role. Despite having similar St_η and Sv_η, the glass bubbles, ($d_p = 92\mu$m) have a larger average cluster area than the lycopodium clusters, which are three times smaller in diameter.

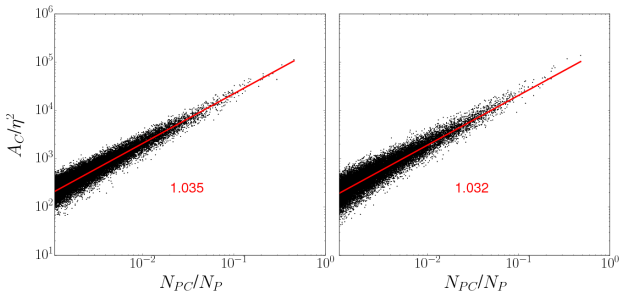

Figure 6. Cluster area normalized by the Kolmogorov area vs. cluster particle counts normalized by the total number of particles in the domain for the (left) $Re_\lambda = 300$, $St_\eta = 1.21$, $Sv_\eta = 0.98$, $\phi_v = 7.72e\text{-}6$ case, and (right) the $Re_\lambda = 500$, $St_\eta = 1.53$, $Sv_\eta = 0.87$, $\phi_v = 5.7e\text{-}7$ case.

Table 1. Clustering experiment parameters

Re_λ	d_p (μm)	St_η	Sv_η	ϕ_v	$\langle C_C \rangle / C_0$	$\langle A_C \rangle / \eta^2$
300	29	1.2	1.0	7.7e-07	8.83	267.1
300	92	0.4	0.3	3.4e-05	3.86	173.9
300	30	0.6	0.5	9.1e-06	3.71	25.8
300	29	1.2	1.0	1.4e-06	5.20	307.3
300	52	3.6	3.0	5.1e-06	8.09	264.5
300	52	3.6	3.0	3.4e-06	8.43	445.4
500	29	1.5	0.9	5.7e-07	9.82	324.5
500	52	4.6	2.6	6.3e-06	7.18	323.3
500	52	4.6	2.6	1.5e-05	7.03	764.9

Particle Settling

We also investigated how turbulence affects particle settling velocity, whether inside clusters or not. Figure 7 shows the ratio between the average measured settling velocity and the theoretical still-fluid terminal velocity vs. St_η, with colors indicating the bulk volume fraction. In agreement with previous studies we observe the maximum settling velocity increase for particles with St_η close to one. The interaction with turbulence increases the settling velocity of these particles by up to three times, similar to results from Good *et al.* (2014) and Aliseda *et al.* (2002). The settling increase is lessened for particles with $St_\eta < 1$, as is the case for lycopodium, and $St_\eta > 1$ as seen for the 52 and 95 μm glass microspheres. We even observe a settling decrease for our largest St_η particles of up to 40%. Good *et al.* (2014) also observed a decrease in settling velocity for the largest particles in their experiments.

We also examined whether preferential sweeping is a plausible mechanism to explain increased settling. In figure 8, the local concentration is conditionally averaged on the vertical fluid velocity, itself normalized by the particle terminal velocity. We count

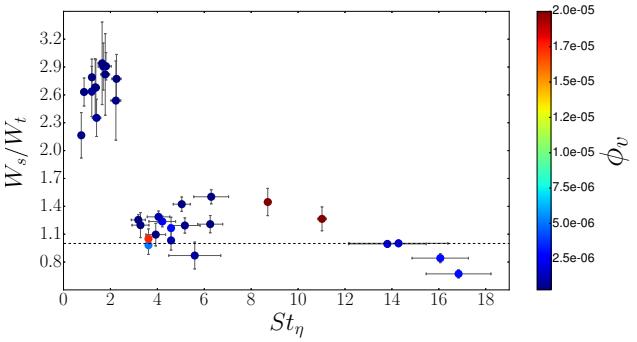

Figure 7. Change in settling velocity over the terminal value, vs. particle Stokes number. Colors indicate bulk volume fraction

the number of particles in each PIV interrogation window, and bin those based on the local value of the vertical fluid velocity, W_f. The concentration is then the number of particles counted for each bin, divided by the sum of the window areas associated to that bin. Finally, the conditionally averaged concentration is normalized by the global particle concentration for all particles and clustered particles, respectively. Figure 8 shows that while all particles are more likely to be in regions of downward sweeping fluid, the effect is especially pronounced for particles in clusters. This raises the question as to what extent clustered particles exert a collective drag on the carrier fluid, possibly adding to the preferential sweeping and settling rate (Bosse *et al.*, 2006), but also how they affect the underlying turbulence.

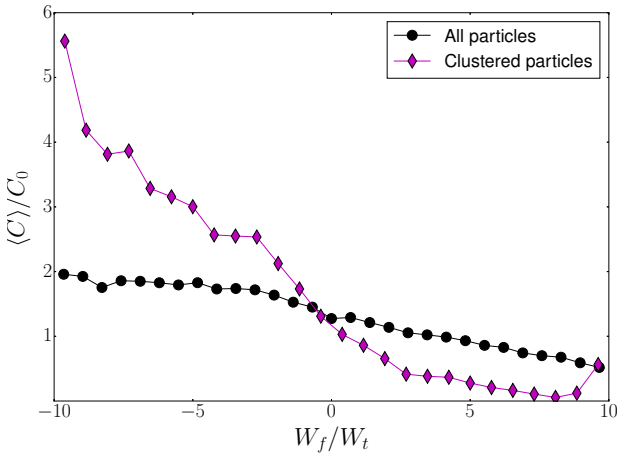

Figure 8. Local concentration for settling particles within clusters and outside of them for a $St_\eta = 3.6$, $Sv_\eta = 2.7$ case.

Back-reaction on carrier fluid

The threshold for two-way coupling, when the particles affect the fluid phase turbulence, is ambiguous and the distinction between one and two-way coupled flows can be clearly made only when the particle back-reaction is included or excluded in a numerical simulation. Some level of two-way coupling is unavoidable in physical system, and the question is rather whether our measurement approach is sensitive enough to accurately quantify it. Here, we evaluate whether the fluid turbulent kinetic energy (TKE) changes between multiphase and single-phase flows. To that end, we took turbulent kintetic energy measurements of both single and multiphase

flows for each Reynolds number. Carter *et al.* (2016) demonstrated the repeatability of our turbulence generation, and thus we can be fairly confident that subsequent runs will be comparable. The large source of uncertainty though lies in the multiphase experiments. Inertial particles displace the tracers that we need to measure the flow velocity, and thus the higher the volume fraction, the less reliable the fluid measurement will be. Therefore we limited our measurements of turbulent kinetic energy in multiphase experiments to relatively low volume fractions, $< 2\text{x}10^{-6}$.

Figure 9 shows the measured TKE for a given multiphase experiment, normalized by the base TKE of the underlying turbulence. There is significant scatter and uncertainty, but there is a general increasing trend, despite the relatively modest volume fractions presented here. There is also no clear separation between one and two-way coupled flows. Particles with large Sv_η travel almost ballistically through the turbulence and simulations by Frankel *et al.* (2016) showed these settling particles can indeed increase TKE. Our findings corroborate those results experimentally, although the limited volume fraction considered in Fig. 8 (one order of magnitude smaller than what considered by Frankel *et al.* (2016)) results in a more modest modification of TKE. Like in the case of settling velocity change, there is no simple relationship between volume fraction, Sv_η and change in turbulent kinetic energy which again emphasizes that there are many parameters influencing the momentum coupling.

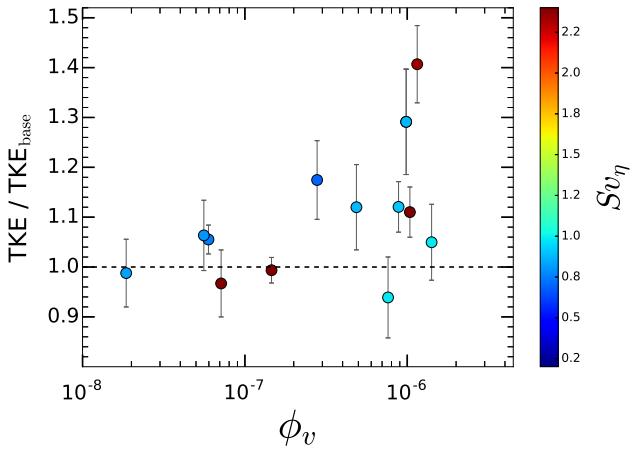

Figure 9. Turbulent kinetic energy of carrier-phase fluid normalized by single phase value for different bulk volume fractions.

Conclusions

We investigated inertial particles falling through homogeneous air turbulence with particular focus on preferential concentration, particle settling velocity and back-reaction on the turbulence itself. Our novel experimental facility generates a region of homogeneous turbulence with negligible mean flow much larger than the integral length scale of the flow. Importantly, this enables the particles to interact with all the scales of the turbulent flow, thereby removing any bias from the turbulence forcing. We use PIV and PTV to find particle and fluid velocities, and when the volume fraction is relatively modest we are able to measure both simultaneously. All experiments were conducted with sub-Kolmogorov particles, but by varying the particle type and turbulence intensity we are able to examine a range of St_η from 0.4 to 17.

We use Voronoï tessellation to find particles sufficiently dense to be considered clusters, but impose a further condition that takes into account the self-similar nature of the underlying turbulence. Clusters are only considered dynamically relevant if they are large enough to exhibit self-similarity as deduced from their size distribution and the fractal nature of their delimiting perimeter.

The clusters we observe frequently exceed the turbulence integral length scale, and on rare occasions we find "megaclusters" up to 30 cm in length. These clusters have areas 10^5 times greater than the Kolmogorov area, η^2. We also find that the cluster concentration is approximately constant over the full range of cluster sizes, meaning that concentration does not depend on size, but on the physical parameters. Between the nine experiments presented here, the cluster concentration ranges from four to ten times greater than the concentration of the full domain, with St_η near one particles exhibiting the most clustering. We also find that the mean cluster size increases with St_η and Sv_η, although the finite-size of particles certainly plays a role in this trend.

Our investigation into particle settling through turbulence found an increase up to three times the still-fluid value for St_η near one. Conditioning the local particle concentration on the average vertical fluid velocity reveals that particles are more likely to be in regions of downward-moving flow as the preferential sweeping mechanism predicts. The effect is even greater for clustered particles, warranting further investigation of how clusters affect the carrier fluid through a collective drag, possibly enhancing preferential sweeping and settling velocity. For our largest St_η, we do observe two cases of particle settling velocity being reduced, but more examination is needed before we can attribute it to a certain cause.

Finally, for relatively small volume fractions where simultaneous fluid and particle velocity measurement is possible, we measured the fluid turbulent kinetic energy. Even for these modest volume fractions, we do find turbulent kinetic energy generally increasing when compared to the single-phase value, illustrating that some degree of two-way coupling is intrinsic to any physical system. However there is significant scatter in our data, which points to the fact that this is a multi-parameter problem so more work is needed to determine what the most relevant parameters are. Bulk volume fraction may be too coarse a parameter, particularly for the heavily-clustered flows where local concentration varies widely in space.

REFERENCES

Aliseda, A. and Cartellier, A. and Hainaux, F. and Lasheras, J.C. 2002 Effect of preferential concentration on the settling velocity of heavy particles in homogeneous isotropic turbulence. *J. Fluid Mech.* **468**, 77–105.

Baker, Lucia, Frankel, Ari, Mani, Ali & Coletti, Filippo 2017 Coherent clusters of inertial particles in homogeneous turbulence. *Submitted* .

Bec, J, Biferale, L, Boffetta, G, Celani, A, Cencini, M, Lanotte, A, Musacchio, S & Toschi, F 2006 Acceleration statistics of heavy particles in turbulence. *J. Fluid Mech.* **550**, 10.

Bec, Jeremie, Homann, Holger & Ray, Samriddhi Sankar 2014 Gravity-driven enhancement of heavy particle clustering in turbulent flow. *Phys. Rev. Lett.* **112** (18), 6–9.

Bellani, Gabriele & Variano, Evan A 2014 Homogeneity and isotropy in a laboratory turbulent flow. *Exp. Fluids* **55** (1).

Bosse, Thorsten, Kleiser, Leonhard & Meiburg, Eckart 2006 Small particles in homogeneous turbulence: Settling velocity enhancement by two-way coupling. *Phys. Fluids* **18** (2), 1–17.

Bragg, Andrew D & Collins, Lance R 2014 New insights from comparing statistical theories for inertial particles in turbulence: I. Spatial distribution of particles. *New J. Phys.* **16**.

Carter, Douglas, Petersen, Alec, Amili, Omid & Coletti, Filippo

2016 Generating and controlling homogeneous air turbulence using random jet arrays. *Exp. Fluids* **57** (12), 1–15.

Cuzzi, Jeffrey N, Hogan, Robert C, Paque, Julie M & Dobrovolskis4, Anthony R 2001 Size-selective concentration of chondrules and other small particles in protoplanetary nebula turbulence. *Astrophys. J.* **546**, 496–508.

Eaton, J K & Fessler, J R 1994 Preferential concentration of particles by turbulence. *Internatinoal J. Multiph. Flow* **20** (94), 169–209.

Elghobashi, S. & Trusdell, G. C. 1993 On the two-way interaction between homogeneous turbulence and dispersed solid particles. I. Turbulence modification. *Phys. Fluids A Fluid Dyn.* **5** (7), 1790–1801.

Ferenc, Járai Szabó & Néda, Zoltán 2007 On the size distribution of Poisson Voronoi cells. *Phys. A Stat. Mech. its Appl.* **385** (2), 518–526.

Frankel, Ari, Pouransari, H, Coletti, F & Mani, A 2016 Settling of heated particles in homogeneous turbulence. *J. Fluid Mech.* **792**, 869–893.

Good, G. H., Ireland, P. J., Bewley, G. P., Bodenschatz, E., Collins, L. R. & Warhaft, Z. 2014 Settling regimes of inertial particles in isotropic turbulence. *J. Fluid Mech.* **759**.

Goto, Susumu & Vassilicos, J. C. 2006 Self-similar clustering of inertial particles and zero-acceleration points in fully developed two-dimensional turbulence. *Phys. Fluids* **18** (11).

Goto, Susumu & Vassilicos, J C 2008 Sweep-stick mechanism of heavy particle clustering in fluid turbulence. *Phys. Rev. Lett.* **100** (5).

Grabowski, Wojciech W. & Wang, Lian-Ping 2013 Growth of Cloud Droplets in a Turbulent Environment. *Annu. Rev. Fluid Mech.* **45** (1), 121005161233001.

Hassan, Y A, Blanchat, T K & Jr, C H Seeley 1992 PIV flow visualisation using particle tracking techniques. *Meas. Sci. Technol.* **3** (7), 633.

Khalitov, D. A. & Longmire, E. K. 2002 Simultaneous two-phase PIV by two-parameter phase discrimination. *Exp. Fluids* **32** (2), 252–268.

Kiger, K. T. & Pan, C. 2000 PIV Technique for the Simultaneous Measurement of Dilute Two-Phase Flows. *J. Fluids Eng.* **122** (December 2000), 811.

Maxey, M R 1987 The gravitational settling of aerosol particles in homogeneous turbulence and random flow fields. *J. Fluid Mech.* **174** (174), 441.

Monchaux, R, Bourgoin, M & Cartellier, A 2010 Preferential concentration of heavy particles: A Voronoï analysis. *Phys. Fluids* **22** (10).

Nemes, András, Lo Jacono, David, Blackburn, Hugh M. & Sheridan, John 2015 Mutual inductance of two helical vortices. *J. Fluid Mech.* **774**, 298–310.

Nielsen, Peter 1993 Turbulence Effects on the Settling of Suspended Particles. *J. Sediment. Res.* **Vol. 63** (5), 835–838.

Poelma, C., Westerweel, J. & Ooms, G. 2007 Particlefluid interactions in grid-generated turbulence. *J. Fluid Mech.* **589**, 315–351.

Sreenivasan, K. 1991 Fractals And Multifractals In Fluid Turbulence. *Annu. Rev. Fluid Mech.* **23** (1), 539–600.

Sundaram, Shivshankar & Collins, Lance R 1997 Collision statistics in an isotropic particle-laden turbulent suspension. Part 1. Direct numerical simulations. *J. Fluid Mech.* **335**, 75–109.

Tooby, P F, Wick, G L & Isaacs, J D 1977 The motion of a small sphere in a rotating velocity field; a possible mechanism for suspending particles in turbulence. *J. Geophys. Res.* **82** (15), 2096–2100.

Variano, Evan a. & Cowen, Edwin a. 2008 A random-jet-stirred turbulence tank. *J. Fluid Mech.* **604**, 1–32.

Wang, L.-P. & Maxey, M. R. 1993 Settling velocity and concentration distribution of heavy particles in homogeneous isotropic turbulence. *J. Fluid Mech.* **256**, 27–68.

Yang, T. S. & Shy, S. S. 2003 The settling velocity of heavy particles in an aqueous near-isotropic turbulence. *Phys. Fluids* **15** (4), 868–880.

Yang, T. S. & Shy, S. S. 2005 Two-way interaction between solid particles and homogeneous air turbulence: particle settling rate and turbulence modification measurements. *J. Fluid Mech.* **526**, 171–216.